Diurnal changes in urban boundary layer environment induced by urban greening

Environmental Research Letters

LETTER

Diurnal changes in urban boundary layer environment induced by urban greening

Jiyun Song and Zhi-Hua Wang[1]

School of Sustainable Engineering and the Built Environment, Arizona State University, PO Box 875306, Tempe, AZ 85287-5306, USA

[1] Author to whom any correspondence should be addressed.

E-mail: zhwang@asu.edu

Keywords: landscape planning, mitigation and adaptation, urban green infrastructure, urban boundary layer

OPEN ACCESS

RECEIVED
9 March 2016

REVISED
4 October 2016

ACCEPTED FOR PUBLICATION
26 October 2016

PUBLISHED
11 November 2016

Abstract

Urban green infrastructure has been widely used for mitigating adverse environmental problems as well as enhancing urban sustainability of cities worldwide. Here we develop an integrated urban-land-atmosphere modeling framework with the land surface processes parameterized by an advanced urban canopy model and the atmospheric processes parameterized by a single column model. The model is then applied to simulate a variety of forms of green infrastructure, including urban lawns, shade trees, green and cool roofs, and their impact on environmental changes in the total urban boundary layer (UBL) for a stereotypical desert city, viz. Phoenix, Arizona. It was found that green roofs have a relatively uniform cooling effect proportional to their areal coverage. In particular, a reduction of UBL temperature of 0.3 °C and 0.2 °C per 10% increase of green roof coverage was observed at daytime and nighttime, respectively. In contrast, the effect of greening of street canyons is constrained by the overall abundance of green infrastructure and the energy available for evapotranspiration. In addition, the increase in urban greening causes boundary-layer height to decrease during daytime but increase at nighttime, leading to different trends of changes in urban air quality throughout a diurnal cycle.

1. Introduction

As dwelling places of more than 50% of global population, urban areas have attracted numerous research efforts and practical concerns for their direct and indirect impacts on hydroclimate, ecosystem, energy consumption, landscape modification, and human health (Arnfield 2003, Georgescu *et al* 2014). One of the major concerns is the excessive thermal stress in cities resulting from prominent urban phenomena such as the heat island effect and extreme heatwaves (Oke 1973, Bowler *et al* 2010, Wilhelmi and Hayden 2010, Schatz and Kucharik 2015). An effective way of mitigating the thermal stress is to 'green' the urban areas by increasing vegetation fraction at neighborhood, city and regional scales (Li *et al* 2005, Gill *et al* 2007, Bowler *et al* 2010). For example, city parks with sizable vegetation covers usually cool the park area and the surrounding built environment (Yu and Hien 2006, Oliveira *et al* 2011). On the other hand, it is the concentrated built areas where people spend most of their time in working and living (Alexandri and Jones 2008). The most popular way of urban greening is to vegetate envelopes of buildings, such as implementation of green roofs and walls (Alexandri and Jones 2008, Pérez *et al* 2011, Yang and Wang 2014a), or to increase the abundance of vegetation in the built environment with parks, lawns and sidewalk trees (Spronken-Smith and Oke 1998, Yu and Hien 2006).

Urban vegetation is effective in mitigating thermal stress, buffering stormwater, and fostering a healthy and friendly living environment, especially for arid cities by creating an 'oasis' (Yu and Hien 2006, Susca *et al* 2011). Vegetation and manmade materials differ significantly in hydrological, thermal, and aerodynamic properties, and therefore interact with the overlying atmospheric boundary layers (ABL) through different mechanisms (Bowler *et al* 2010, Song and Wang 2015a, 2015b). The main cooling mechanism of vegetation is via altering the surface energy partitioning through evapotranspiration (ET). The enhanced

ET can effectively redistribute available energy (mainly the net radiation) at the land surface into latent heat, leading to reduced sensible heat for heating the overlying atmosphere (Yang and Wang 2014b). In addition, urban trees can provide shading to roads, building walls, and partial rooftops, cooling the built environment through interception of direct and diffuse radiative heat exchange (Chow and Brazel 2012, Wang *et al* 2016).

Urban greening has significant impact on the thermal environment in the urban canopy layer (roughly from the ground to the average roof level) by modifying land surface energy and water transport processes, which in turn modulates the thermal environment in the urban boundary layer (UBL) (from the rooftop level to a few kilometers in elevation). In particular, two types of urban heat island (UHI) need to be differentiated when urban green infrastructure is used for mitigating the UHI effect, viz. the urban canopy heat island and UBL heat island (Oke 1976). Most recent urban environmental studies are focused on the thermal environment in the urban canopy layer (Georgescu *et al* 2014, Li *et al* 2014) since it is directly related to the thermal comfort of urban residents. While UBL dynamics are relatively under-explored, and in-depth analysis is hitherto lacking (Sharma *et al* 2016), they are of crucial importance by interfacing the built environment with large-scale phenomena ranging from synoptic to global scales (Arnfield 2003, Seneviratne and Stöckli 2008). Moreover, the impact of urban greening extends via land-atmosphere interactions and boundary-layer flow not only spatially (from local to global scale) but also temporally (from event to climate scale); a recent example is found in tracing the rainfall pattern in Africa to Asian irrigation through changes in Asian monsoon (de Vrese *et al* 2016).

The objective of this study is to assess the impact of different urban greening strategies on UBL dynamics, particularly boundary-layer temperature and height. This study adds to the existing studies by bridging the gap by extending the locality in urban canopy layer studies to boundary layer environment, hence linking urban hotspots to global change at large. Recent urban environmental studies incorporating boundary-layer dynamics were mostly based on mesoscale weather prediction models such as the weather research and forecasting (WRF) model (Georgescu *et al* 2014, Li *et al* 2014, Sharma *et al* 2016). While comprehensive physics of land-atmosphere interactions can be captured by the fully-integrated mesoscale models, we hypothesize that it is practically difficult to disentangle the effect of individual dynamic modules (e.g. subsurface transport, plant biophysics, radiation parameterization, atmospheric schemes, etc) and their relative contribution to the final signal in environmental changes. This is largely due to the uncertainty challenge in mesoscale modeling inherent in complex model structures, large parameter space, and coupling of multiple dynamic modules (Hargreaves 2010, Song and Wang 2016), which in turn leads to the outstanding challenge faced in this study that 'How can the impact of landscape greening on the urban environment be singled out from that of the complexity of total environmental physics?'

To address the aforementioned question, here we developed a stand-alone model for urban-land-atmosphere interactions and applied it to simulate the diurnal urban surface energy transport processes and UBL dynamics. The coupled model constitutes of an advanced single-layer urban canopy model (SLUCM) with realistic representation of green infrastructure (Wang *et al* 2013, Wang 2014a, Yang *et al* 2015), as well as a single column model (SCM) for parameterization of diurnal ABL dynamics under both convective and stable conditions (Troen and Mahrt 1986, Noh *et al* 2003, Hong 2010). The integrated numerical tool is used to simulate the impact of representative types of urban green infrastructure including lawns, trees, and vegetated roofs over various landscapes on the local thermal environment at both the surface and the boundary layers. With these applications, the current study is expected to provide useful guidelines for city planners and practitioners in adopting sustainable urban planning and mitigation strategies. In particular, it will be shown that urban greening via its impact on the UBL evolution has significant implications to the environmental quality in cities, such as environmental cooling via heat dispersion in the UBL and improvement of air quality via regulation of the UBL height.

2. Methodology

2.1. Urban land-atmosphere modeling framework

In this section, the development of a novel urban land-atmosphere modeling framework is presented that resolves the diurnal evolution of UBL dynamics. The UBL is well mixed at daytime due to strong convection and turbulence, but is stably stratified at night since the land surface is cooler than the atmosphere (Stull 1988). The UBL dynamics will be resolved by the SCM based on a modified *K*-theory (Troen and Mahrt 1986, Noh *et al* 2003, Hong *et al* 2006, Hong 2010). In the SCM, the boundary layer will be resolved in two different schemes, i.e. convective and stable in accordance with typical daytime and nighttime dynamics. The governing turbulence diffusion equations of the virtual potential temperature for the convective boundary layer (CBL) (Troen and Mahrt 1986) and the stable boundary layer (SBL) (Garratt and Brost 1981) are given by

$$\frac{\partial \theta_v}{\partial t} = \frac{\partial(-\overline{w'\theta'_v})}{\partial z}, \tag{1}$$

$$\frac{\partial \theta_v}{\partial t} = \frac{\partial(-\overline{w'\theta'_v})}{\partial z} + \frac{1}{\rho_a c_p}\frac{\partial F_N}{\partial z}, \tag{2}$$

respectively, where θ_v is the virtual potential temperature, i.e. the boundary-layer atmospheric temperature with pressure (*potential*) and humidity (*virtual*) corrections, and is hereafter referred to as UBL temperature for brevity, $\overline{w'\theta'_v}$ the vertical kinematic eddy heat flux, F_N the net longwave radiative flux, and ρ_a and c_p the density and specific heat of air, respectively.

The vertical eddy heat flux at the lowest level of the SCM is given by

$$(\overline{w'\theta'_v})_s = \frac{H_s}{\rho_a c_p}, \quad (3)$$

where H_s is the surface heat flux calculated by the SLUCM. It is noteworthy that there is an alternative group of urban parameterization schemes using the multi-layer canopy model and more sophisticated representations of three-dimensional (3D) environmental flow (Taha 2008, Gutiérrez *et al* 2015a, 2015b). As our focus in this study is on the interfacing of scalar (heat and moisture) fluxes between the urban canopy and boundary layers, the predictive skills of the single-layer model on scalar transport is comparable with those of multi-layer schemes (Chen *et al* 2011). The primary reason that we selected the single layer scheme in this study is due to its numerical simplicity and relative computational economy. In the SLUCM, the generic urban surface energy balance equation over a built terrain is given by

$$R_n + A_F - G_0 = H_s + LE_s, \quad (4)$$

where R_n, H_s and LE_s are the net radiative, sensible and latent heat respectively, A_F the anthropogenic heat, and G_0 the ground heat flux. Sensible and latent heat fluxes from the whole urban canopy are estimated as the aggregation of heat fluxes arising from individual urban facets in the canopy layer, viz. roofs, walls, and ground surfaces. For example, the total surface sensible heat flux is given by (Wang *et al* 2013)

$$H_s = r\sum_{k=1}^{2} f_{R,k} H_{R,k} + w\sum_{k=1}^{2} f_{G,k} H_{G,k} + 2hH_W, \quad (5)$$

where r, h, and w are the normalized roof width, building height and road width respectively; subscripts R, G, and W stand for roof, ground, and wall (i.e. the three main urban canyon facets) respectively; and f is the areal fraction of each urban sub-facet k. For example, $f_{R,2}$ and $f_{G,2}$ can represent the areal fractions of green or white roof systems.

The vertical eddy heat flux at the top boundary condition of the SCM, i.e. at the UBL top when $z = z_h$ is given by (Hong 2010)

$$(\overline{w'\theta'_v})_{z_h} = -0.15\left(\frac{\theta_{v1}}{g}\right) w_m^3 / z_h, \quad (6)$$

where θ_{v1} is the virtual potential temperature at the lowest model level, w_m the velocity scale and z_h the boundary layer height. For a CBL, z_h is positively related to surface heating by an analytical equation (Ouwersloot and de Arellano 2013), whereas for a SBL, z_h is derived through a simple prognostic growth rate equation which implicitly accounts for the radiative cooling and is negatively related to sensible heat (Yamada 1979). A more detailed formulation of evolution of the boundary layer height, the surface heat flux (kinematic), and the diffusivity coefficients is listed in table 1.

2.2. Model evaluation

The urban land-atmospheric modeling framework introduced in the above section is evaluated by comparisons against field measurements. Surface energy budgets (i.e. R_n, H_s, LE_s) in the pre-monsoon period from 13 June to 30 June, 2012 in west Phoenix site (33°29′1.9″N, 112°08′33.4″W) (detailed site and instrumentation information can be found in Chow *et al* 2014) are used to test the stand-alone SLUCM, with the comparison between simulations and measurements shown in figure 1(a). Model predicted results are in good agreement with the field measurements, with RMSE values of 23.8, 55.3, and 47.4 W m^{-2} for R_n, H_s, LE_s respectively, indicating that the SLUCM is capable of prediction of surface energy budgets with reasonable accuracy. In the ABL, results of the virtual potential temperature profiles as predicted by the offline SCM simulations are compared with two sets of recorded field measurements: the first set is on 1–2 July, 2005 at Point Reyes site (38° 5′ 27.6′ N, 122° 57′ 25.80′ W) in California, USA and the second on Wangara Day 33 at Hay site (34° 30′ S, 144° 56′ E) in New South Wales, AUS as shown in figures 1(b) and (c) respectively. The simulated virtual potential temperature profiles agree well with the field measurements at both sites (detailed site and instrumentation information can be found in Clarke *et al* 1971 and Holdridge *et al* 2011), with RMSE values of 0.1 K, 0.4 K at 21:27 pm and 09:32 am respectively over Point Reyes site in California and RMSE values of 0.7 K, 0.5 K, 0.4 K, 0.3 K at 00:19 am, 03:25 am, 12:00 pm, 15:00 pm respectively over the Hay site in New South Wales. At last, the coupled SLUCM-SCM was used to predict the virtual potential temperature profiles at an east Phoenix site (33° 27′ N, 111° 57′ W). The predicted temperature profile in 2 July, 2013 is compared with the field data from the NOAA/ESRL radiosonde database (Schwartz and Govett 1992) as shown in figure 1(d). As the radiosonde measurements were rarely recorded below 300 m in elevation, i.e. within a typical nocturnal boundary layer, comparison is made here between model simulations and field measurements for daytime, where the RMSE value is 0.5 K for the comparison in figure 1(d).

2.3. Urban greening scenarios

In this study, we select the Phoenix Metropolitan Area in the State of Arizona, USA as our testbed. Located in the northeast of the Sonoran Desert, Phoenix is known for its mild winters with mean temperature of 10 °C and hot summers with mean temperature of 32 °C (Baker *et al* 2002). This area consists of a wide variety

Table 1. Parameterization schemes for convective and stable boundary layers.

Variables	CBL	SBL
Kinematic fluxes	$-\overline{w'x'} = K_x\left(\frac{\partial x}{\partial z} - \gamma_x\right) - \overline{(w'x')}_{z_h}\left(\frac{z}{z_h}\right)^3$ (Hong 2010)	$-\overline{w'x'} = K_x\frac{\partial x}{\partial z} - \overline{(w'x')}_{z_h}\left(\frac{z}{z_h}\right)^3$ (Hong 2010)
Eddy diffusivity	$K_c = P_r^{-1}kw_m z\left(1 - \frac{z}{z_h}\right)^2$ (Hong *et al* 2006)	$K_c = kw_m z\left(1 - \frac{z}{z_h}\right)^2$ (Hong 2010)
Velocity scale	$w_m = \left(u_*^3 + \frac{8kw_{*b}^3 z}{z_h}\right)^{1/3}$ (Hong *et al* 2006)	$w_m = u_*$ (Hong 2010)
ABL height	$z_h = \left\{ \begin{array}{l} z_{h0}^2 + \frac{(2\ +\ 4w_e)}{\gamma_{\theta v}} \\ \left[\Delta\theta_{v,0} z_{h0}^{\frac{1+w_e}{w_e}} - \left(\frac{w_e}{1\ +\ 2w_e}\right)\gamma_{\theta v} z_{h0}^{\frac{1+2w_e}{w_e}}\right] \\ \times\left(\hat{z}_h^{-\frac{1}{w_e}} - z_{h0}^{-\frac{1}{w_e}}\right) + \left(\frac{2\ +\ 4w_e}{\gamma_{\theta v}}\right)\int_{t_0}^{t}(\overline{w'\theta_v'})_s dt \end{array} \right\}^{1/2}$ (Ouwersloot and de Arellano 2013)	$z_h(t) = z_h(t-1) - \frac{\Delta t}{\theta_h - \theta_s}\left[2Cz_h\frac{\partial\theta_s}{\partial t} - z_h\frac{\partial\theta_s}{\partial t} + 4(\overline{w'\theta_v'})_s\right]$ (Yamada 1979)

Notes: z_h is the boundary-layer height, w the vertical velocity scale, u_* the friction velocity, $\gamma_{\theta v}$ the lapse rate in the free atmosphere, θ_v the virtual potential temperature, K_c the eddy diffusivity, γ the non-local mixing term, P_r the Prandtl number, k the von Karman constant, and subscripts '0', 'b', 's', 'm', 'h', 'e' denoting at the initial stage, corrected by incorporating moisture, on the surface, in the mixed-layer, at the boundary-layer top, and in the entrainment respectively.

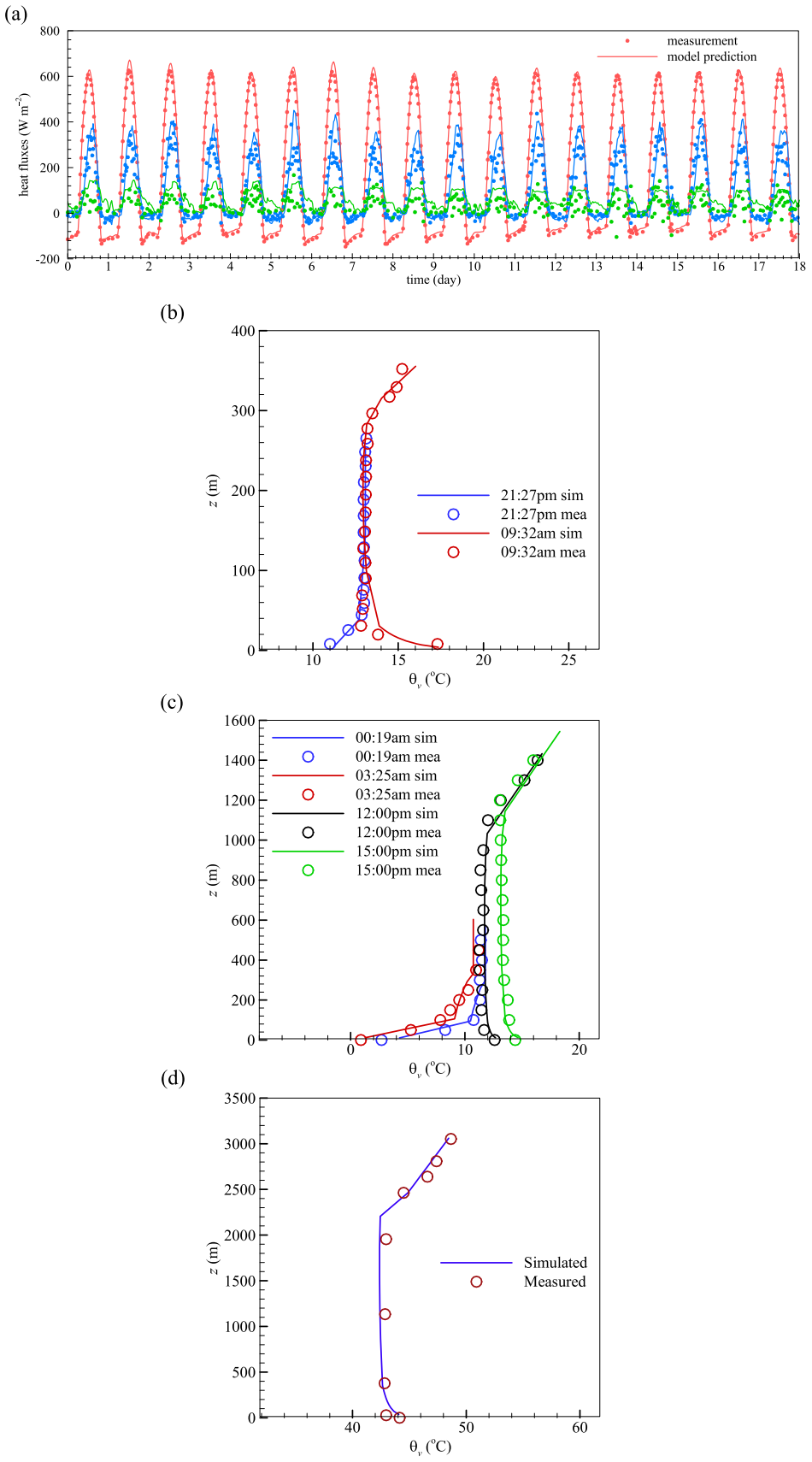

Figure 1. Comparison of field measurements with model simulation results: (a) surface energy fluxes at Phoenix AZ, including radiation R_n (red), sensible heat flux H_s (blue), and latent heat flux LE_s (green) 13–30 June 2012; (b) UBL temperature θ_v at 21:27 on 1 July, 2005 and 09:32 on 2 July, 2005 (Local time) at Point Reyes CA, (c) θ_v at 00:19, 03:25, 12:00, 15:00 (Local time) on Wangaran Day 33 at Hay site, New South Wales, Australian; and (d) θ_v at 16:30 (Local time) on 2 July, 2013 in Phoenix AZ.

Figure 2. Four typical landscapes in Phoenix, Arizona: (a) desert, (b) mesic, (c) xeric, and (d) oasis landscapes.

of heterogeneous landscapes, including not only remnant desert and 'gray' (buildings, roads, parking lots, etc) landscapes, but also large green landscapes (mesic lawns, xeric trees, golf courses, urban lakes, etc) for the sake of amenity, recreation, ecosystem service, stormwater harvesting, and urban heat mitigation (Baker *et al* 2002, Foster *et al* 2011, EPA 2013). In particular, there are four common types of residential landscape in Phoenix (see figure 2), including desert (with little or no vegetation, and no irrigation system), xeric vegetation (plants that require drip irrigation systems with low water use, e.g. native desert trees), mesic (non-native plants such as lawns that require sprinkler irrigation systems with high water use), and oasis (a combination of xeric tree and mesic lawn) landscapes (Yabiku *et al* 2008).

In the subsequent context, this numerical model framework will be applied to simulate different scenarios of green infrastructure in the Phoenix metropolitan area, driven by summer meteorological conditions with cloud-free sunny days from 13 June to 30 June, 2012. The baseline scenario consists of the set of (i) various xeric tree crown radii ranging from 0 to 1 m with an interval of 0.2 m, (ii) various mesic lawn fraction ranging from 0% to 50% with an interval of 10%, and (iii) various green roof coverage ranging from 0% to 50% areal fraction with an interval of 10%. The range of parameters is determined from practical concerns of deployment of urban green infrastructure in the study area (e.g. EPA 2013, Wang *et al* 2016). In total, we test nine combinations of green infrastructure strategies (see table 2), including Scenarios (a), (b), (c) with nominal (as in the baseline scenario) variation of xeric trees and mesic lawns, and 0%, 25%, and 50% green roof fraction respectively, Scenarios (d), (e), (f) with nominal variation of urban lawns and green roofs, and tree crown size of 0 m, 0.5 m, and 1 m respectively, and Scenarios (g), (h), (i) with nominal variation of trees and green roofs, and mesic lawns of 0%, 25%, and 50% lawn coverage, respectively. The intercomparison of simulated results of these scenarios is presented in figures 3–6, where the subplot captions are identical to the scenario numbers.

Table 2. Description of the nine scenarios of urban greening.

Scenario #	Tree crown radius (m)	Lawn fraction (%)	Green roof fraction (%)
a	[0, 1]	[0, 50]	0
b	[0, 1]	[0, 50]	25
c	[0, 1]	[0, 50]	50
d	0	[0, 50]	[0, 50]
e	0.5	[0, 50]	[0, 50]
f	1	[0, 50]	[0, 50]
g	[0, 1]	0	[0, 50]
h	[0, 1]	25	[0, 50]
i	[0, 1]	50	[0, 50]

3. Results and discussion

3.1. Impact on boundary-layer temperature

Figures 3 and 4 show the impact of urban greening on the UBL thermal states, measured in terms of maximum and minimum UBL temperature respectively, averaged from the top of urban canopy layer to the top of UBL. Comparing figures 3 and 4 clearly shows that the cooling effect of urban green infrastructure is more significant during daytime than nighttime. Despite the

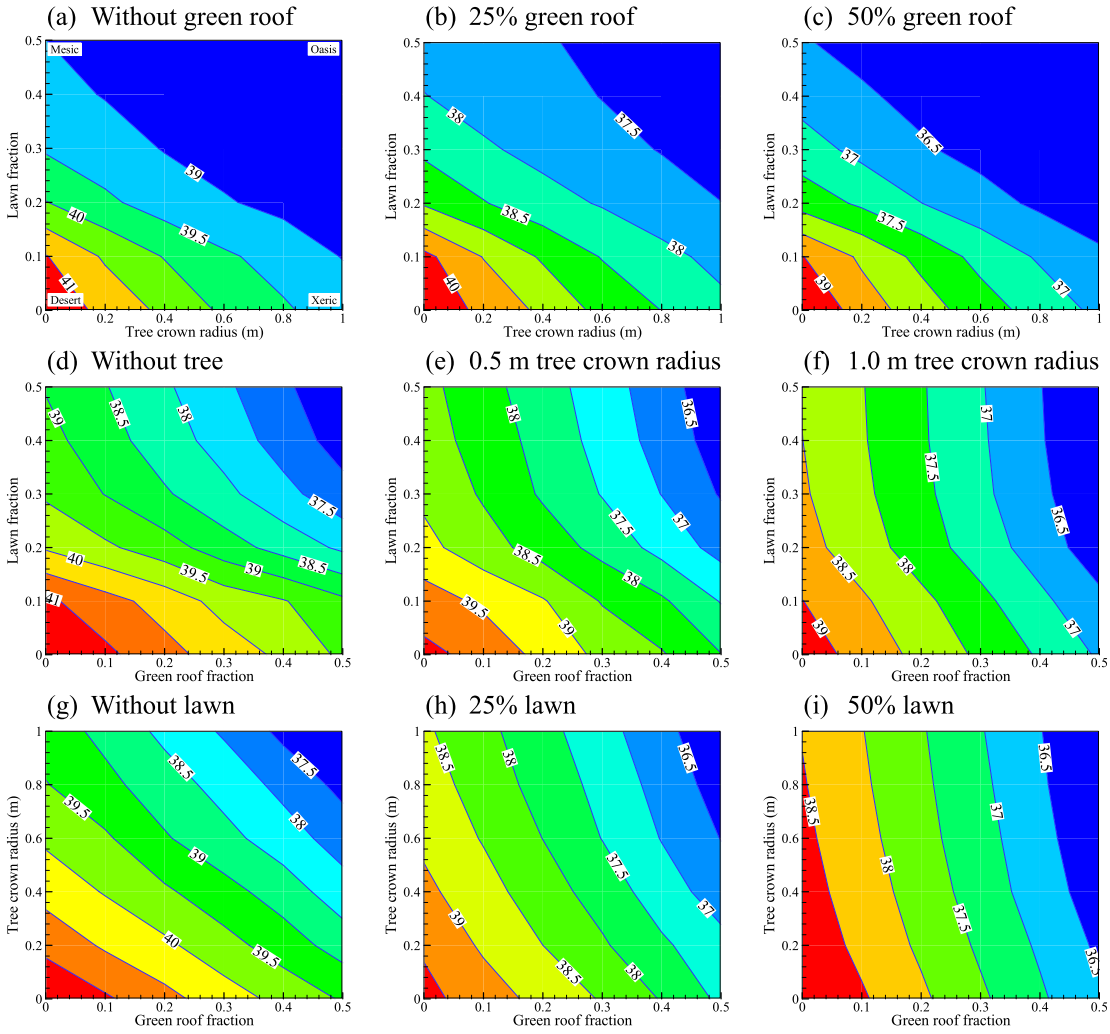

Figure 3. Comparison of daily maximum UBL temperature (°C) for different urban greening scenarios: the numbering of subplots corresponds to that of urban greening scenarios. Note that the mean UBL temperature is averaged throughout the mixed layer.

mechanisms of different urban vegetation in re-distributing the surface energy balance (evaporative cooling by lawns and green roofs and radiative shading by xeric trees), the potential cooling effect is constrained by the ultimate energy incident on urban facets. The absence of solar radiation during nighttime therefore ultimately limits the potential cooling effect of all forms of urban mitigation strategies, leading to less surface cooling, which in turn circumscribes the air temperature reduction in the nocturnal UBL.

The first rows, viz. figures 3 and 4(a)–(c) clearly indicate that the cooling effect of green roofs is significant over all different landscapes. For a desert landscape (with no lawn or tree coverage), the maximum UBL temperature $\theta_{v,max}$ reduces by 1 °C per 25% green roof fraction increment, while the minimum UBL temperature $\theta_{v,min}$ decreases 0.6 °C and 0.4 °C, with green roof coverage increased from 0% to 25% and from 25% to 50%. For an oasis landscape (with maximum urban lawns and trees), every 25% increase of roof greening reduces $\theta_{v,max}$ by 1 °C–1.5 °C, and $\theta_{v,min}$ by 0.6 °C. Similarly, for xeric (slighter wetter than desert) and mesic (slighter drier than oasis) landscapes, the same degree of roof greening leads to a similar amount of cooling. The cooling effect of roof greening can also be seen from figures 3 and 4(d)–(i), where the distribution of contours for green roof fractions $f_{v,R}$ is roughly uniform in all these subplots, indicating a relatively uniform UBL cooling rate (0.5 °C at daytime and 0.2 °C at nighttime) per constant 10% increase of green roof coverage. Similar linear cooling effect of green roof on surface temperature has been reported in earlier studies (e.g. Yang and Wang 2014a). But the current study identifies that uniform cooling by green roofs can 'penetrate' from urban surface into the overlying UBL under both stable and unstable conditions.

Unlike green roofs, the cooling effect of urban vegetation in street canyons, viz. mesic lawns and shade trees, is apparently limited by the abundance of total vegetation cover. This can be seen from the change of contour patterns for lawns in figures 3 and 4(d)–(f), and for trees in figures 3 and 4(g)–(i), which is more prominent during nighttime. For example, when there is no green roof, greening urban canyons with 50% mesic lawn can effectively reduce $\theta_{v,max}$ and

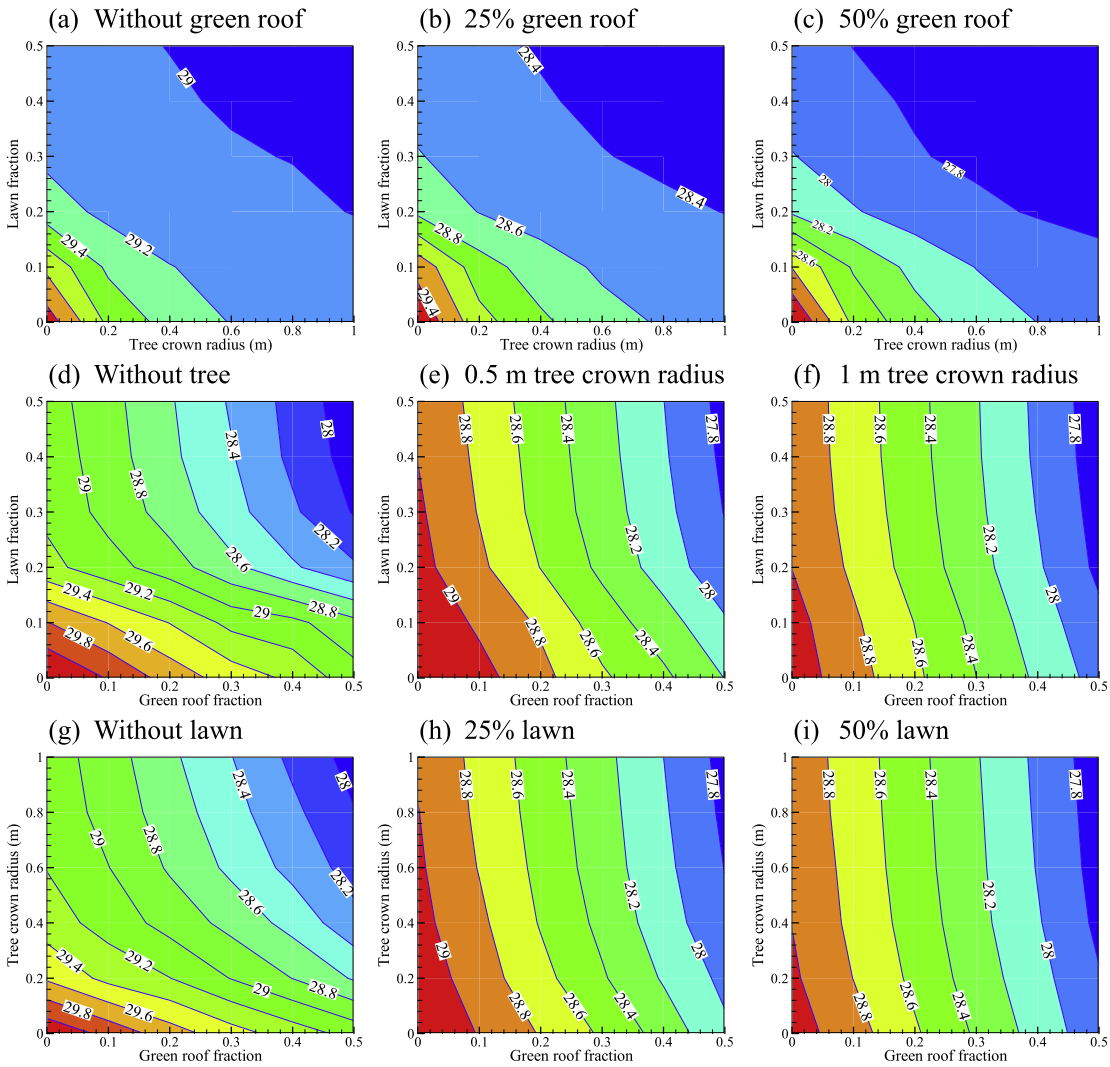

Figure 4. As figure 3 but for minimum mean UBL temperature (°C).

$\theta_{v,min}$ by 2.5 °C and 1.0 °C respectively when no shade tree is present in the canyon (figures 3(d) and 4(d)), whereas with the presence of shade trees of 1 m crown radii, the cooling effect of the same amount of lawn coverage decreases drastically to around 0.5 °C and 0.2 °C for $\theta_{v,max}$ and $\theta_{v,min}$ respectively (figures 3(f) and 4(f)). A similar degree of reduced UBL cooling effect is also observed for xeric landscape with or without the presence of lawns (see figures 3 and 4(g) with 3 and 4(i)). This phenomenon of constrained cooling effect in the UBL by urban lawns and trees in street canyons is consistent with that of the surface temperature (Wang *et al* 2016), which can be attributed to the competition for available energy by increases in grass richness, tree shading, and nocturnal radiative cooling.

3.2. Impact on boundary-layer height

The impact of urban greening on the evolution of UBL height for convective (daytime) and stable (nocturnal) boundary layers is shown in figures 5 and 6, respectively. As the evolution of the UBL height is strongly modulated by the surface thermal state and upwelling (mainly sensible) fluxes (Song and Wang 2015a), it is expected that patterns of the contour plots in figures 5 and 6 follow closely those in figures 3 and 4. In general, the overall degree of modification of the UBL height by green infrastructure is greater in daytime than that in nighttime, again attributable to the magnitude of absolute amount of available energy. Furthermore, with increased degree of urban greening, the CBL height shrinks (figure 5) whereas the SBL height increases (figure 6). The underlying physics is that urban green infrastructure reduces uprising surface sensible heat flux that is positively related to the CBL height but negatively correlated with the SBL height (Yamada 1979, Ouwersloot and de Arellano 2013).

The modification of UBL dynamics by urban greening has strong implications for urban air quality and human health. Firstly, the typical UBL height is ~O (1 km) at daytime, but ~O (100 m) during nighttime. In addition, the daytime boundary layer is highly convective, featuring strong turbulent mixing that favors pollutant dispersion. In contrast, the nocturnal

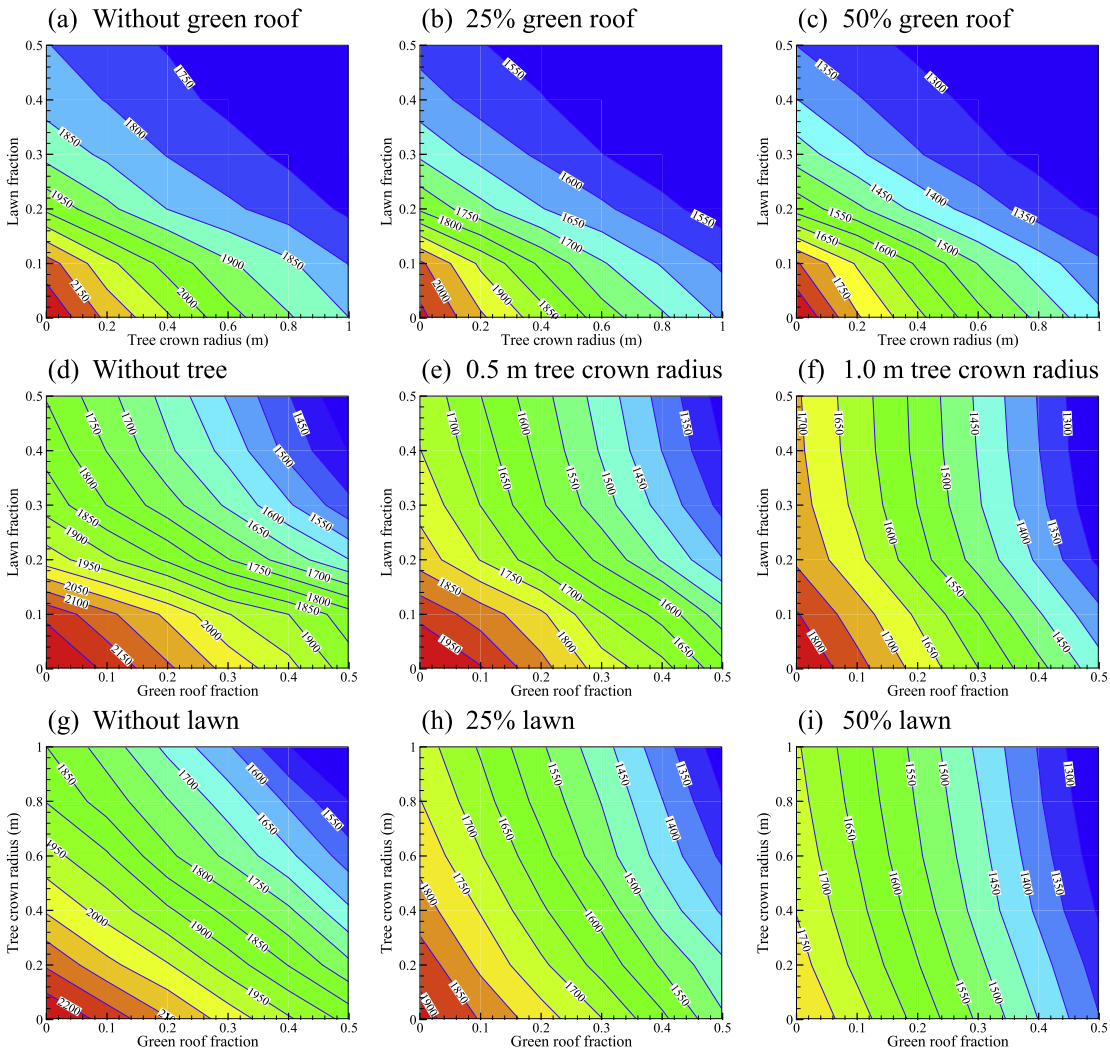

Figure 5. As figure 3 but for the maximum daytime boundary layer height (m).

boundary layer is relatively stable and causes accumulation of pollutants (Stull 1988). Due to a shallower boundary layer and more stable atmosphere, gaseous pollutants, particulate matters, and other scalars (such as carbon dioxide) produced at the land surface tend to stagnate over a built environment at night, leading to severe degradation of environmental quality. With urban greening, the UBL height decreases at daytime but increases at nighttime. Pollutant concentration at daytime could be increased due to a shallower boundary layer and weakened vertical mixing (Sharma *et al* 2016). However, pollutant concentration at nighttime could be reduced due to a deeper boundary layer. Apart from the indirect influence on improving nocturnal air quality, urban green infrastructure directly impacts air quality by absorbing the deposition of atmospheric pollutants (Currie and Bass 2008, Pugh *et al* 2012). To accurately quantify the impact of green infrastructure on urban air quality, the coupling of both physical and bio-chemical processes is required and needs interdisciplinary research efforts (Tzoulas *et al* 2007, Yang *et al* 2008).

In addition, the impact of different urban vegetation on ABL height change varies, similar to their influence on the ABL thermal structure. The effect of green roofs is relatively independent of the urban greening in canyons, and remains effective in modulating both CBL and SBL heights in a relatively uniform rate of increase with green roof coverage. For example, an increase of 50% green roof coverage leads to the reduction of CBL height by 350 m, 350 m, 450 m, and 450 m (figures 5(a)–(c)), as well as increase of SBL height by 70 m, 120 m, 130 m, and 130 m (figures 6(a)–(c)), over desert, xeric, mesic, and oasis landscapes respectively.

In contrast, urban-greening in the street canyon level is not as effective as green roof systems in a desert city for all landscape types. For example, urban trees of 0.5 m radius can change the CBL height by 250 m (decrease) and the SBL height by 80 m (increase) over a desert landscape (figures 5 and 6(d), (e)), whiles over an oasis landscape (with 50% lawns), the changes of the CBL and SBL heights by the same trees are reduced to 100 m and 20 m, respectively (figures 5 and 6(e), (f)). It follows that (i) the boundary-layer structure is

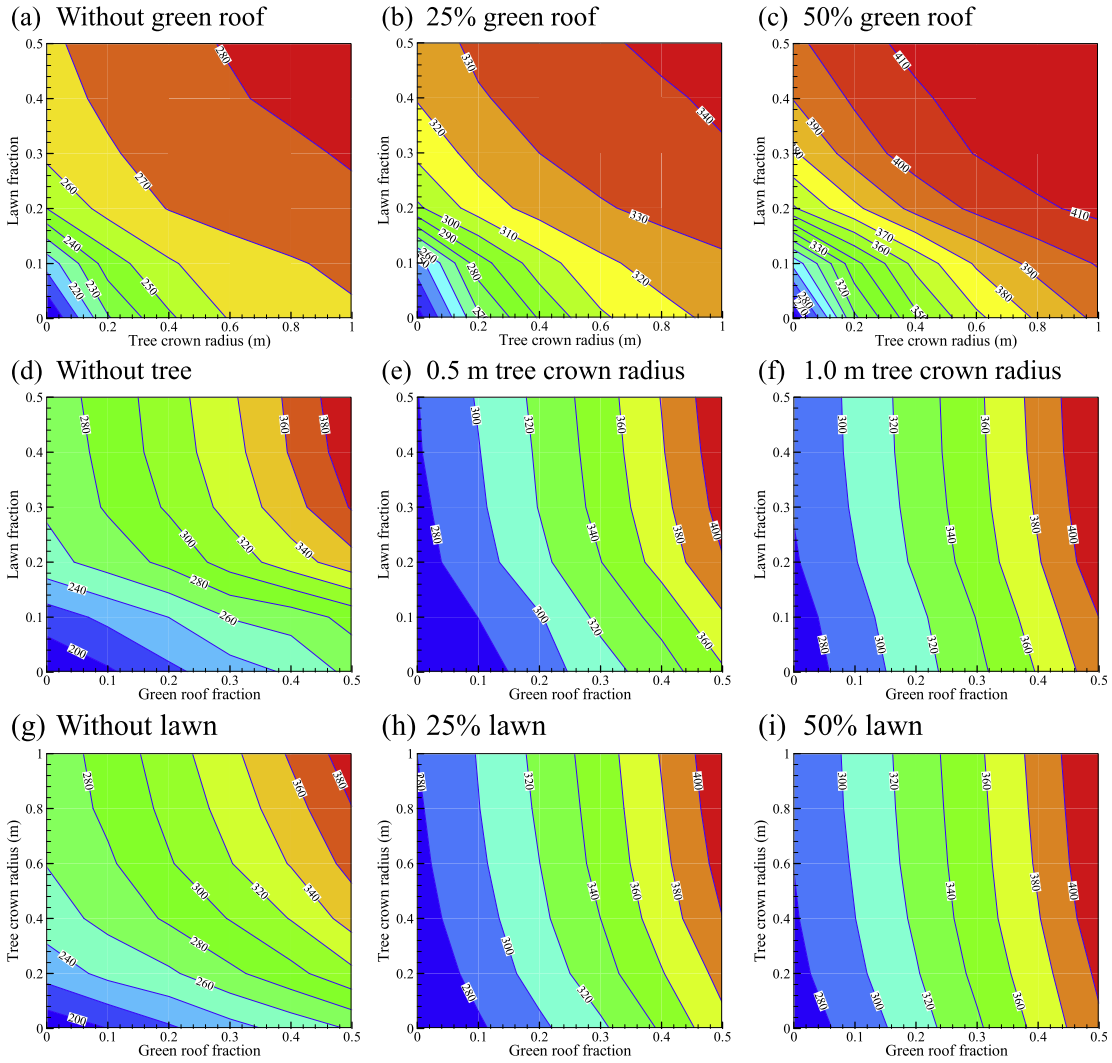

Figure 6. As figure 3 but for maximum nighttime boundary layer height (m).

more susceptible to urban trees over desert landscapes than those over oasis landscapes; and (ii) the CBL height is more sensitive to tree crown sizes than the SBL. In street canyons, the shading effect (blockage of direct solar radiation) of trees dominates during daytime, whereas the longwave trapping effect (multiple reflections of diffusive radiation) is overwhelming during nighttime (Wang 2014a). Similar to trees, the effect of urban lawns in regulating UBL heights is also constrained by the overall degree of greening in street canyons, largely resembling their impact on ABL temperatures (see section 3.1). It also follows that adding urban lawns is more effective in regulating ABL height over xeric than mesic landscapes.

3.3. Comparison of green and white roof systems

In addition to the intercomparison of different forms of urban vegetation, green (vegetated) and white (highly reflective) roofs are two popular strategies to mitigate urban heat stress (Sailor *et al* 2011, Akbari *et al* 2012). To compare the cooling effect of green and white roofs on the UBL, we study in this section 10 additional scenarios with green/white roof coverage fractions ranging from 0% to 90% with 10% interval, driven by meteorological conditions in 13–30 June, 2012 at Phoenix. The impact of these roof systems on ABL temperatures is shown in figure 7. While both green and white roofs decrease both daytime and nocturnal ABL temperatures, the evaporative cooling by green roofs, when adequately irrigated (with nearly saturated soil water content so that the cooling efficiency will not be constrained by water availability), is found to be more significant than the reflective cooling of white roofs. It is noteworthy that under calm and clear nocturnal conditions, surface cooling of both roof systems is mainly driven by net longwave radiation and retarded by the thermal properties of the subsurface materials to release the stored heat (Sproken-Smith and Oke 1999), while cooling of the overlying SBL is mainly dominated by heat flux divergence (Garratt and Brost 1981). For both roofs, the cooling effect is less significant at night due to less available energy supply than that of daytime. The evaporative cooling by green roofs in summer,

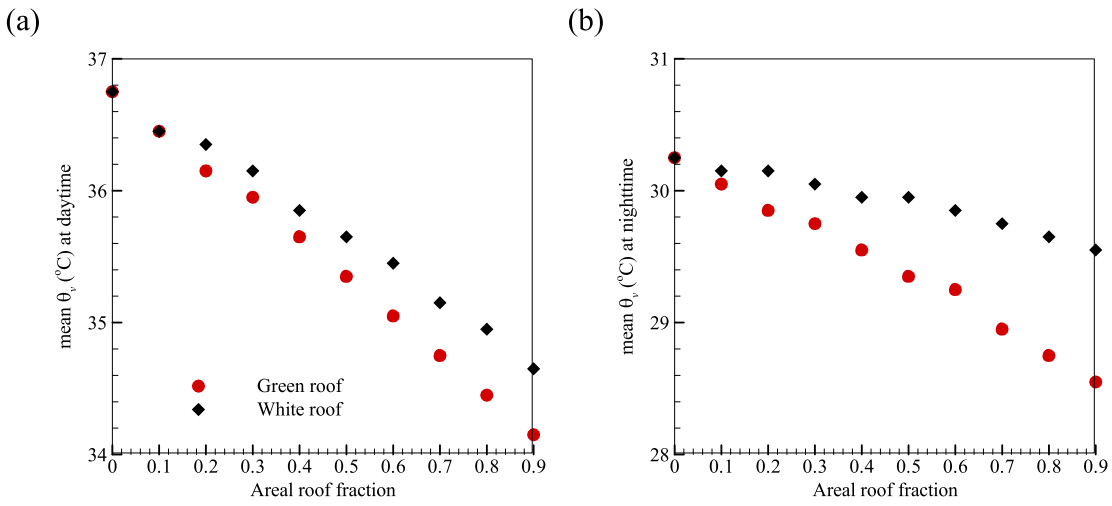

Figure 7. Intercomparison of the cooling effect of green and white roofs on (a) mean daytime UBL temperature θ_v (°C) and (b) mean nighttime UBL temperature θ_v (°C), as functions of areal roof fraction.

especially in arid cities, leads to a reduction of 1.6 °C mean nocturnal UBL temperature, compared to 0.7 °C nocturnal cooling by white roofs which is mainly a residual effect due to the diminished thermal storage by daytime cooling as albedo has no effect at night since there is no shortwave radiation.

4. Concluding remarks

This study evaluates the impact of urban green infrastructure on UBL dynamics over a variety of landscapes using a coupled land-surface-atmosphere modeling framework. In general, we found that the implementation of green infrastructure is effective in regulating the thermal states of the UBL, mainly via the re-partitioning of the urban land surface energy balance and the resulting surface cooling. Constrained by the supply of available energy, the effect of urban greening, specifically on temperature and boundary-layer height, is more significant on the convective atmospheric layers during daytime than the stable ones. It is also found that the effect of roof cooling, by vegetation or use of reflective materials, is roughly proportional to the degree of roof greening (viz. the areal fraction of coverage), and remains effective despite the presence of urban vegetation in street canyons. However, vegetated roof has a greater cooling capacity than reflective roof especially at nighttime. In particular, the coverage of 90% vegetated roof lead to additional ~1 °C than the reflective roof of same fractional coverage. On the other hand, the cooling effect of urban lawns and shade trees depends on the status quo of urban greening and the overall abundance of green infrastructure in the neighborhood. The marginal effect of increasing urban lawns and trees diminishes with the total vegetation coverage as well as the soil moisture state (i.e. they are more effective over desert/xeric than over mesic/oasis landscapes). With the presence of big trees, the cooling effect of added lawn will be significantly restrained. It is noteworthy that with little demand of water via the drip irrigation system, xeriscaping trees present a promising urban mitigation strategy as an alternative to more traditional water-demanding urban lawns. This is particularly attractive to house-owners and city planners in an arid or semi-arid environment like Phoenix.

Moreover, note that the modeling framework used in this study resolves the vertical transport processes of heat and scalars in the soil-surface-atmosphere continuum. As our focus is on alleviating surface- and boundary-layer thermal stress, this model setting helps to single out the impact of landscape modification and is representative of calm and clear weather conditions with a UBL dominated by free convection; these conditions are particularly relevant for our study of a desert valley city. On the other hand, we also offer the caveat that the current modeling framework is limited by its inadequacy in capturing the horizontal advection and synoptic wind shear effects. This constraint can be released by integrating the current model into a mesoscale numerical weather model with predictive capabilities, such as the WRF model; the possibility remains open for extending the current research to more realistic representation of cities with a variety of climatic, geographic, and socio-economic conditions.

Acknowledgments

This work is supported by the US National Science Foundation (NSF) under grants CBET-1435881 and CBET-1444758. The NOAA/ESRL/Global Systems Division is acknowledged for providing the sounding data at the Phoenix AZ site.

References

Akbari H, Matthews H D and Seto D 2012 The long-term effect of increasing the albedo of urban areas *Environ. Res. Lett.* **7** 024004

Alexandri E and Jones P 2008 Temperature decreases in an urban canyon due to green walls and green roofs in diverse climates *Build. Environ.* **43** 480–93

Arnfield A J 2003 Two decades of urban climate research: a review of turbulence, exchanges of energy and water, and the urban heat island *Int. J. Climatol.* **23** 1–26

Baker L A, Brazel A J, Selover N, Martin C, McIntyre N, Steiner F R, Nelson A and Musacchio L 2002 Urbanization and warming of phoenix (Arizona, USA): impacts, feedbacks and mitigation *Urban Ecosyst.* **6** 183–203

Bowler D E, Buyung-Ali L, Knight T M and Pullin A S 2010 Urban greening to cool towns and cities: a systematic review of the empirical evidence *Lands. Urban Plan.* **97** 147–55

Chen F *et al* 2011 The integrated WRF/urban modelling system: development, evaluation, and applications to urban environmental problems *Int. J. Climatol.* **31** 273–88

Chow W T and Brazel A J 2012 Assessing xeriscaping as a sustainable heat island mitigation approach for a desert city *Build. Environ.* **47** 170–81

Chow W T, Volo T J, Vivoni E R, Jenerette G D and Ruddell B L 2014 Seasonal dynamics of a suburban energy balance in Phoenix, Arizona *Int. J. Climatol.* **34** 3863–80

Clarke R H, Dyer A J and Scientific C 1971 *The Wangara Experiment: Boundary Layer Data* (Australia: CSIRO) 362 pp

Currie B A and Bass B 2008 Estimates of air pollution mitigation with green plants and green roofs using the UFORE model *Urban Ecosys.* **11** 409–22

De Vrese P, Hagemann S and Claussen M 2016 Asian irrigation, African rain: remote impacts of irrigation *Geophys. Res. Lett.* **43** 3737–45

EPA 2013 Green infrastructure barriers and opportunities in Phoenix, Arizona—an evaluation of local codes and ordinances

Foster J, Lowe A and Winkelman S 2011 The value of green infrastructure for urban climate adaptation, Center for Clean Air Policy

Garratt J R and Brost R A 1981 Radiative cooling effects within and above the nocturnal boundary layer *J. Atmos. Sci.* **38** 2730–46

Georgescu M, Morefield P E, Bierwagen B G and Weaver C P 2014 Urban adaptation can roll back warming of emerging megapolitan regions *Proc. Natl Acad. Sci.* **111** 2909–14

Gill S, Handley J, Ennos A and Pauleit S 2007 Adapting cities for climate change: the role of the green infrastructure *Built Environ.* **33** 115–33

Gutiérrez E, González J E, Martilli A, Bornstein R and Arend M 2015a Simulations of a heat-wave event in New York City using a multilayer urban parameterization *J. Appl. Meteor. Climatol.* **54** 283–301

Gutierrez E, Martilli A, Santiago J L and Gonzalez J E 2015b A mechanical drag coefficient formulation and urban canopy parameter assimilation technique for complex urban environments *Bound.-Layer Meteorol.* **157** 333–41

Hargreaves J C 2010 Skill and uncertainty in climate models *Wiley Interdiscip. Rev. Clim. Change.* **1** 556–64

Holdridge D, Ritsche M, Prell J and Coulter R 2011 Balloon-Borne Sounding System (SONDE) Handbook *Report No. DOE/SC-ARM/TR-029* U.S. Department of Energy, Washington DC 27 pp

Hong S 2010 A new stable boundary-layer mixing scheme and its impact on the simulated East Asian summer monsoon *Q. J. R. Meteorol. Soc.* **136** 1481–96

Hong S Y, Noh Y and Dudhia J 2006 A new vertical diffusion package with an explicit treatment of entrainment processes *Mon. Weather Rev.* **134** 2318–41

Li D, Bou-Zeid E and Oppenheimer M 2014 The effectiveness of cool and green roofs as urban heat island mitigation strategies *Environ. Res. Lett.* **9** 055002

Li F, Wang R, Paulussen J and Liu X 2005 Comprehensive concept planning of urban greening based on ecological principles: a case study in Beijing, China *Lands. Urban Plan.* **72** 325–36

Noh Y, Cheon W, Hong S and Raasch S 2003 Improvement of the K-profile model for the planetary boundary layer based on large eddy simulation data *Bound.-Layer Meteorol.* **107** 401–27

Oke T R 1973 City size and the urban heat island *Atmos. Environ.* **7** 769–79

Oke T R 1976 The distinction between canopy and boundary-layer urban heat islands *Atmosphere* **14** 268–77

Oliveira S, Andrade H and Vaz T 2011 The cooling effect of green spaces as a contribution to the mitigation of urban heat: a case study in Lisbon *Build. Environ.* **46** 2186–94

Ouwersloot H and de Arellano J V-G 2013 Analytical solution for the convectively-mixed atmospheric boundary layer *Bound.-Layer Meteorol.* **148** 557–83

Pérez G, Rincón L, Vila A, González J M and Cabeza L F 2011 Green vertical systems for buildings as passive systems for energy savings *Appl. Energy* **88** 4854–9

Pugh T A, MacKenzie A R, Whyatt J D and Hewitt C N 2012 Effectiveness of green infrastructure for improvement of air quality in urban street canyons *Environ. Sci. Technol.* **46** 7692–9

Sailor D J, Elley T B and Gibson M 2011 Exploring the building energy impacts of green roof design decisions—a modeling study of buildings in four distinct climates *J. Build. Phys.* **35** 372–91

Schatz J and Kucharik C J 2015 Urban climate effects on extreme temperatures in Madison, Wisconsin, USA *Environ. Res. Lett.* **10** 094024

Schwartz B and Govett M 1992 A hydrostatically consistent North American radiosonde data base at the forecast systems laboratory , 1946—present *NOAA Technical Memorandum* NOAA Forecast System Laboratory, Boulder

Seneviratne S I and Stöckli R 2008 The role of land-atmosphere interactions for climate variability in Europe *Climate Variability and Extremes During the Past 100 years* (Netherlands: Springer) pp 179–93

Sharma A, Conry P, Fernando H J S, Hamlet A F, Hellmann J J and Chen F 2016 Green and cool roofs to mitigate urban heat island effects in the Chicago metropolitan area: evaluation with a regional climate model *Environ. Res. Lett.* **11** 064004

Song J and Wang Z-H 2015a Impacts of mesic and xeric urban vegetation on outdoor thermal comfort and microclimate in Phoenix, AZ *Build. Environ.* **94** 558–68

Song J and Wang Z-H 2015b Interfacing the urban land–atmosphere system through coupled urban canopy and atmospheric models *Bound.-Layer Meteorol.* **154** 427–48

Song J and Wang Z-H 2016 Evaluating the impact of built environment characteristics on urban boundary layer dynamics using an advanced stochastic approach *Atmos. Chem. Phys.* **16** 6285–301

Spronken-Smith R A and Oke T R 1998 The thermal regime of urban parks in two cities with different summer climates *Int. J. Remote Sens.* **19** 2085–104

Spronken-Smith R A and Oke T R 1999 Scale modelling of nocturnal cooling in urban parks *Bound.-Layer Meteorol.* **93** 287–312

Stull R B 1988 *An Introduction to Boundary Layer Meteorology* (Dordrecht : Kluwer) 666 pp

Susca T, Gaffin S and Dell'Osso G 2011 Positive effects of vegetation: Urban heat island and green roofs *Environ. Pollut.* **159** 2119–26

Taha H 2008 Meso-urban meteorological and photochemical modeling of heat island mitigation *Atmos. Environ.* **42** 8795–809

Troen I and Mahrt L 1986 A simple model of the atmospheric boundary layer; sensitivity to surface evaporation *Bound.-Layer Meteorol.* **37** 129–48

Tzoulas K, Korpela K, Venn S, Yli-Pelkonen V, Kaźmierczak A, Niemela J and James P 2007 Promoting ecosystem and

human health in urban areas using green infrastructure: a literature review *Landscape Urban Plan.* **81** 167–78
Wang Z-H 2014a Monte Carlo simulations of radiative heat exchange in a street canyon with trees *Sol. Energy* **110** 704–13
Wang Z-H 2014b A new perspective of urban–rural differences: the impact of soil water advection *Urban Clim.* **10** 19–34
Wang Z-H, Bou-Zeid E and Smith J A 2013 A coupled energy transport and hydrological model for urban canopies evaluated using a wireless sensor network *Q. J. R. Meteorol. Soc.* **139** 1643–57
Wang Z-H, Zhao X, Yang J and Song J 2016 Cooling and energy saving potentials of shade trees and urban lawns in a desert city *Appl. Energy* **161** 437–44
Wilhelmi O V and Hayden M H 2010 Connecting people and place: a new framework for reducing urban vulnerability to extreme heat *Environ. Res. Lett.* **5** 014021
Yabiku S T, Casagrande D G and Farley-Metzger E 2008 Preferences for landscape choice in a Southwestern desert city *Environ. Behav.* **3** 382–400
Yamada T 1979 Prediction of the nocturnal surface inversion height *J. Appl. Meteorol.* **18** 526–31
Yang J and Wang Z-H 2014a Physical parameterization and sensitivity of urban hydrological models: application to green roof systems *Build. Environ.* **75** 250–63
Yang J and Wang Z-H 2014b Land surface energy partitioning revisited: a novel approach based on single depth soil measurement *Geophys. Res. Lett.* **41** 8348–58
Yang J, Wang Z-H, Chen F, Miao S, Tewari M, Voogt J and Myint S 2015 Enhancing hydrologic modeling in the coupled weather research and forecasting—urban modeling system *Bound.-Layer Meteoro.* **155** 87–109
Yang J, Yu Q and Gong P 2008 Quantifying air pollution removal by green roofs in Chicago *Atmos. Environ.* **42** 7266–73
Yu C and Hien W N 2006 Thermal benefits of city parks *Energy Build.* **38** 105–20